Highly sensitive detection of DNA by electrogenerated chemiluminescence amplification using dendritic $Ru(bpy)_3^{2+}$-doped silica nanoparticles

Se Won Bae, Jeong-Wook Oh, Ik-Soo Shin, Min Sun Cho, Yang-Rae Kim, Hasuck Kim* and Jong-In Hong*

Received 7th October 2009, Accepted 8th January 2010
First published as an Advance Article on the web 21st January 2010
DOI: 10.1039/b920998k

This study describes the development and characterization of a novel dendritic signal amplification strategy. It relies on the use of two different $Ru(bpy)_3^{2+}$-doped silica nanoparticles ($Probe_{1,2}$RSNP and $Probe_{2c}$RSNP) coated with complementary DNAs, which can be simply and conveniently self-assembled to build sandwich-type dendritic architectures on a gold grid. The performance of this dendritic amplification route was demonstrated in conjunction with the electrogenerated chemiluminescent (ECL) detection of the target DNA. Compared to normal amplification, dendritic amplification allowed a 5-fold enhancement of the ECL signals. The higher sensitivity allowed by the dendritic amplification route was attributed to the hybridization between the DNA ($Probe_2$DNA) on $Probe_{1,2}$RSNP (normal amplification) and the complementary DNA ($Probe_{2c}$ DNA) on the additional $Probe_{2c}$RSNP. As low as 1 fM of 22-bp-long target DNA was clearly detected. The experimental results demonstrated that the ECL intensity achieved through dendritic amplification showed a good linear relationship with the concentration of the target DNA over a wide linear range (10 fM∼10 pM).

Introduction

The enormous amount of genetic information brought by extensive genome sequencing has raised the need for simple, fast, cheap and high-throughput miniaturized DNA sensing for clinical diagnosis, pathology, and environmental screening studies. Such DNA sensors conventionally consist of immobilized DNA strands and their complementary counterparts so that the immobilized DNAs capture their complementary targets and the recognition event for the targets is informed as a measurable signal. Various detection methods are applied to achieve signal transduction in DNA biosensors, such as optical methods, evanescent and acoustic wave methods, optical fibers and electrochemical methods.[1–4] Typically, the electrochemical approach to analyze hybridized target DNA provides simple, cost-effective, miniaturized diagnostic tools and also enables highly sensitive detection.[5–7] Among various electrochemical methods, the electrogenerated chemiluminescence (ECL) technique, which involves light generation near an electrode through an electrochemical redox reaction, is very promising because of advantages of both electrochemical and optical techniques.[8–17] The ECL technique has a wide linear range of chemiluminescence and does not require the use of complex and expensive light sources and fluorescent dyes. Recently, nanomaterials (*e.g.*, carbon nanotubes, gold nanoparticles and silica nanoparticles[18–21]) have been used to develop ECL-based ultrasensitive biosensors. For instance, $Ru(bpy)_3^{2+}$-doped silica nanoparticles (RSNPs) exhibited strong luminescent and highly photostable signals because they have a large number of luminophores encapsulated inside rigid silica matrices.[22] Although their use results in excellent signal enhancement in the presence of even a trace amount of target DNA, the development of much more sensitive platforms would still prove indispensible for hybridization-based DNA detection.

In this paper, we present a new DNA sensing protocol based on the use of ECL signal amplification of dendritic RSNPs. The proposed sensing protocol is composed of a two-step scheme; as shown in Fig. 1, target DNA (yellow) is captured on the gold grid that contains capture DNA (blue), which is complementary to the 5′-end of the target DNA. Two types of DNA-coated RSNP—$Probe_{1,2}$RSNP and $Probe_{2c}$RSNP—are employed in our study. $Probe_{1,2}$RSNP is coated with $Probe_2$ DNA and $Probe_1$ DNA (red), which is complementary to the 3′-end of the target DNA. $Probe_{2c}$RSNP is coated with $Probe_{2c}$ DNA (green), which is hybridized with $Probe_2$ DNA present on $Probe_{1,2}$RSNP. Normal amplification is accomplished by the interaction of $Probe_1$ DNA on the $Probe_{1,2}$RSNP with the target DNA captured by the immobilized capture DNA on the gold grid. Dendritic amplification is realized by additional hybridization of $Probe_{2c}$RSNP onto the normally amplified $Probe_{1,2}$RSNP. $Probe_{1,2}$RSNP is hybridized with $Probe_{2c}$RSNP by base pairings between $Probe_2$ DNA of $Probe_{1,2}$ RSNP and $Probe_{2c}$ DNA of $Probe_{2c}$RSNP. Consequently, the target DNA was successfully quantified from 10 fM to 10 pM using our dendritic amplification strategy.

Experimental

1. Reagents and instruments

Oligonucleotides used in the present study were purchased from Bioneer Inc. (Seoul, Korea). Triton X-100, cyclohexane, tris(2,2′-bipyridyl)dichlororuthenium(II)hexahydrate, tri-n-propylamine (TPA), tetraethyl orthosilicate (TEOS), NH_4OH (25–30 wt%), and 1-hexanol were obtained from Sigma-Aldrich. We purchased 3-aminopropyltriethoxysilane (APTES) and disuccinimidyl

Department of Chemistry, College of Natural Science, Seoul National University, Seoul, 151-747, Korea. E-mail: jihong@snu.ac.kr; hasuckkim@snu.ac.kr; Fax: +82 2 889 1568; Tel: +82 2 880 6682

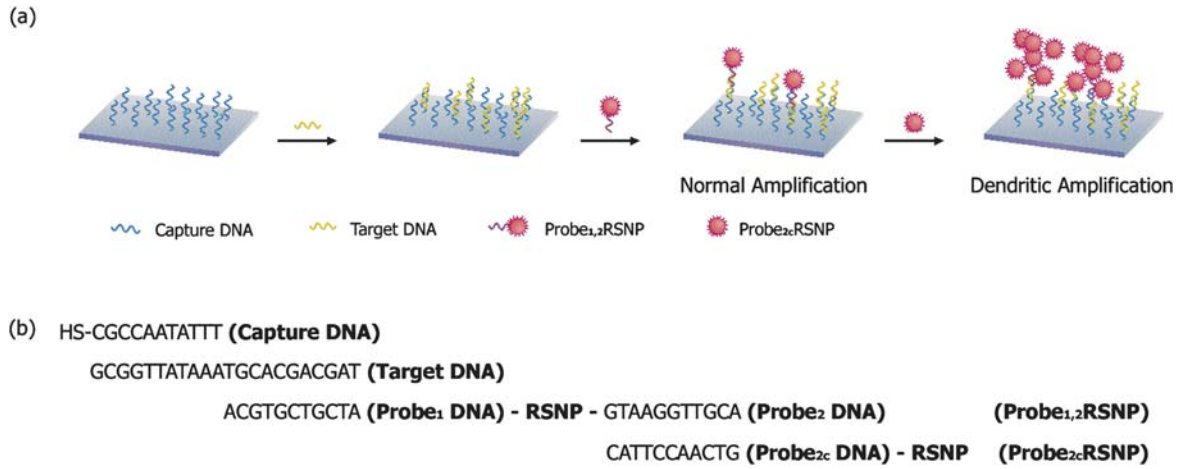

Fig. 1 (a) Schematic illustration of a sandwich DNA assay and its signal amplification based on DNA-conjugated RSNPs. (b) Synthetic DNA sequences and hybridization modes for DNA detection and its signal amplification.

glutarate (DSG) from TCI and Pierce, respectively. Electrochemical measurements were performed in a conventional three-electrode cell with a CHI 660 Electrochemical Analyzer (CHI Inc., Texas). The working electrode was gold-coated (150 nm) on a Si wafer electrode, which was earlier covered with oxide film (300 nm) as an insulator and Ti film (20 nm) as an adhesion layer. Plasma-enhanced chemical vapor deposition using the TEOS source (*P*-5000, Applied Materials, Korea) and e-beam evaporation (Maestek Inc., Korea) was applied to the coating of oxide and metal films, respectively. The gold electrodes were cleaned using piranha solution (95% H_2SO_4/30% H_2O_2, 3 : 1 v/v) before use. A Pt gauze electrode and Ag/AgCl (saturated KCl) were used as the auxiliary and reference electrodes, respectively. The ECL spectrum and intensity were obtained using a charge-coupled device camera (LN/CCD 1752-PB/VSAR, Princeton Instruments, Trenton, NJ) cooled below −110 °C and a photomultiplier tube module (PMT; H6780-20, Hamamatsu, Japan) operating at 0.8 V. The TEM image was taken on a Hitachi H-7600.

2. Preparation of oligonucleotide-conjugated RSNPs

2.1. Synthesis of RSNPs. RSNPs were synthesized using a reverse microemulsion method recently reported by Tan *et al.*[22] In brief, 1.77 mL of Triton X-100, 7.5 mL of cyclohexane, and 1.8 mL of 1-hexanol were mixed by constant magnetic stirring. We then added 400 μL of H_2O and 80 μL of 0.1 M $Ru(bpy)_3^{2+}$ solution, followed by the addition of 100 μL of TEOS. After 30 min of stirring, 60 μL of NH_4OH was added to initiate silica polymerization. After 18 h, the amine-modified silica postcoating procedure was initiated by adding 50 μL of TEOS, 50 μL of APTES, and 30 μL of NH_4OH. After the modification, particles were centrifuged, sonicated, and vortexed four times with 95% ethanol. The particles were then washed once with H_2O.

2.2. Synthesis of $Probe_{1,2}$RSNPs and $Probe_{2c}$RSNPs. To conjugate with amine-modified DNA, the following surface modification steps were performed on the RSNPs (Fig. 2): we activated 2 mg of amine-modified RSNPs by mixing them with 35 mg of DSG in 1.5 ml of 100 mM phosphate-buffered saline (PBS) solution (pH 7.4). After 2 h of stirring at 40 °C, the reaction mixture was centrifuged, sonicated, and vortexed four times with PBS. The final $Probe_{1,2}$RSNPs were synthesized by adding $Probe_1$ DNA and $Probe_2$ DNA (1 : 1 ratio) to the above DSG-modified RSNP solution. After 3 h of stirring at 40 °C, the reaction mixture was washed in the same manner described above. The above procedure was adopted to synthesize $Probe_{2c}$RSNPs with $Probe_{2c}$ DNA (the complementary DNA of $Probe_2$ DNA).

3. Hybridization protocol and ECL detection

Immobilization of capture DNA was performed on the gold electrode (1.0 cm × 0.5 cm) with 180 μL of PBS and 20 μL of 100 μM capture DNA for 2 h at 50 °C and then washed with PBS at 25 °C and dried with N_2 gas. Hybridization of the target DNA was performed with 90 μL of PBS and 10 μL of the target DNA for 1 h at 50 °C and then washed in the same manner as described above. The washed electrode was immersed in 10 μL of $Probe_{1,2}$RSNP solution (1 mg of $Probe_{1,2}$RSNP in 1 mL of PBS) and 90 μL of PBS for 1 h at 50 °C before being washed in the same manner as described above. The resulting electrode was immersed in 10 μL of $Probe_{2c}$RSNP solution (1 mg of $Probe_{2c}$RSNP in 1 mL of PBS) and 90 μL of PBS for 1 h at 50 °C before being washed. The hybridized electrodes were employed as the working electrodes for the ECL measurements. ECL intensities were measured using a homemade ECL cell with a PMT module concomitantly scanning the electrode potential within the range of 0.0 to +1.3 V (*vs.* Ag/AgCl) in 100 mM of PBS containing 10 mM of TPA.

Results and discussion

1. Characterization of RSNP

In standard water-in-oil microemulsion, water nanodroplets are stabilized by surfactants and remain scattered in bulk oil. The nucleation and growth of the silica are mainly regulated by these water nanodroplets. Furthermore, $Ru(bpy)_3^{2+}$ is physically encapsulated in the silica network, which results in the

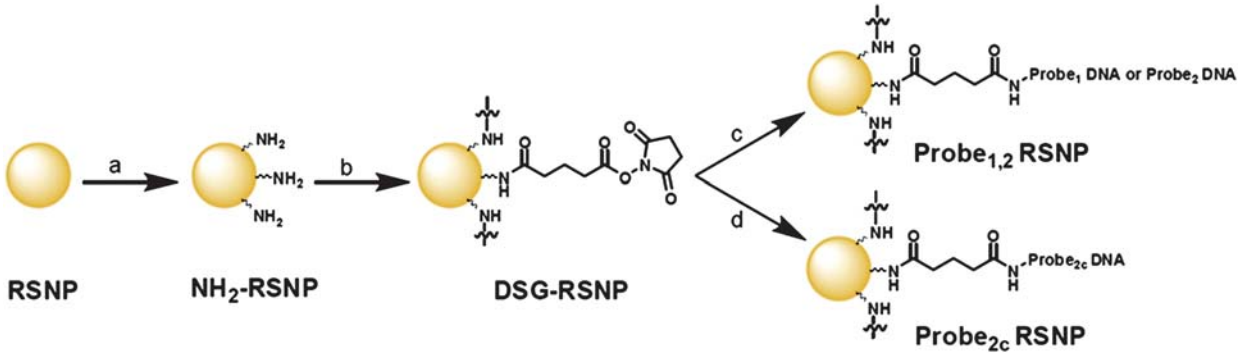

Fig. 2 Synthetic procedure of DNA-conjugated RSNPs. (a) APTES, TEOS and NH_4OH. (b) DSG. (c) $probe_1$ DNA (terminal amine modified) and $probe_2$ DNA (terminal amine modified). (d) $probe_{2c}$ DNA (terminal amine modified).

production of highly monodispersed RSNPs.[23] The RSNPs prepared by this method were consistent in size (~60 nm) and shape, as characterized by the TEM image shown in Fig. 3a.

We were able to introduce thousands of $Ru(bpy)_3^{2+}$ inside each silica nanoparticle, which led to the strong ECL signal as shown in Fig. 3b. The ECL spectrum of RSNPs is nearly the same as that of the free $Ru(bpy)_3^{2+}$ ion in solution, as shown in Fig. 3b. Since TPA is a small molecule, the porous silica matrix could not retard its penetration. On the other hand, although the pore size is bigger than the $Ru(bpy)_3^{2+}$ molecule, $Ru(bpy)_3^{2+}$ could not be leached out from the silica matrix since there is a strong electrostatic interaction between $Ru(bpy)_3^{2+}$ and silica.[24,25]

Fig. 4 illustrates that the cyclic voltammetric behavior and the corresponding ECL curve of the $Probe_{1,2}$RSNPs (normal amplification), which are conjugated to the Au electrode, are similar to those reported before.[21,26,27] Two oxidative peaks appear at 0.34 V and 1.1 V during the positive scan. The small oxidative peak at 0.34 V is attributed to the catalytic oxidation of TPA at the gold surface.[28] When electrode potential is scanned beyond 0.67 V, the thiol monolayer is destroyed due to oxidative desorption of thiol and it leads to the exposure of electroactive site so that the large peak is observed at 1.1 V due to the direct oxidation of TPA and the formation of Au oxide. The subsequent reduction peak at 0.42 V is obtained due to the reduction of Au oxide film.

2. Comparison of dendritic amplification with normal amplification

Fig. 5 shows the ECL behavior of the RSNP-immobilized electrode for the recognition of target DNA hybridization through dendritic

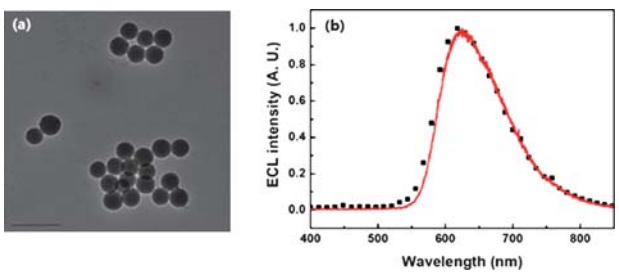

Fig. 3 (a) TEM image of RSNPs (scale bar = 200 nm). (b) Normalized ECL spectra from RSNPs (dotted line) and the free $Ru(bpy)_3^{2+}$ ion (red line) with 10 mM of TPA in 100 mM of PBS solution (pH 7.4).

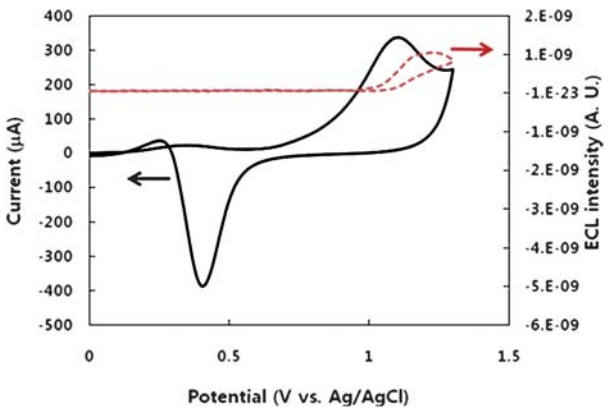

Fig. 4 Cyclic voltammogram (black line) and corresponding ECL (red dotted line) of the $Probe_{1,2}$RSNPs (normal amplification) in the presence of 10 fM target DNA with 10 mM of TPA in 100 mM of PBS solution (pH 7.4). Scan rate: 100 mV s^{-1}.

amplification (—) compared with normal amplification (···). In both cases, the onset potential of ECL is ~0.90 V which corresponds to the direct oxidation of TPA in aqueous solution. It is known that the generation of ECL within the potential range

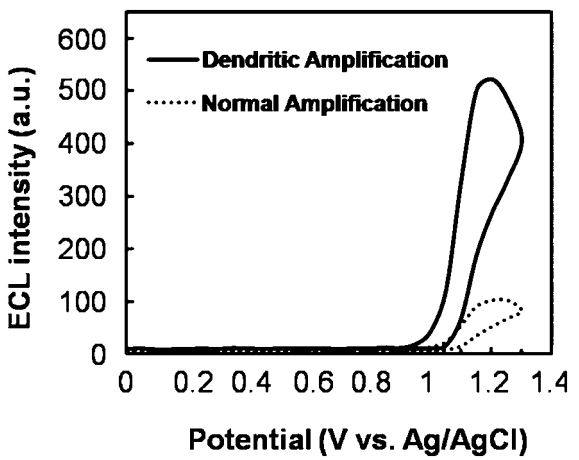

Fig. 5 The ECL profiles for the target DNA hybridized with $Probe_{1,2}$RSNPs (normal amplification, ···) and $Probe_{2c}$RSNPs (dendritic amplification, —). The concentration of the target DNA is 10 fM with 10 mM of TPA in 100 mM of PBS solution (pH 7.4). Scan rate: 100 mV s^{-1}.

before direct oxidation of $Ru(bpy)_3^{2+}$ can be achieved through the TPA cation radical.[24,27] The TPA radical produced presumably electrocatalyzes $Ru(bpy)_3^{2+}$ to $Ru(bpy)_3^{+}$ and subsequently produces $Ru(bpy)_3^{2+*}$ through reacting with the TPA radical. The ECL intensity then increases until it reaches a maximum at ~1.20 V, which is roughly in the range of the oxidation peak potential of $Ru(bpy)_3^{2+}$ at a Au electrode. The direct oxidation of $Ru(bpy)_3^{2+}$ results in intense ECL *via* a "catalytic route" where electrogenerated $Ru(bpy)_3^{3+}$ reacts with the TPA radical.[24] It also implies that our dendritic amplification strategy does not affect any of the ECL routes of dissolved $Ru(bpy)_3^{2+}$ and allows the enhanced ECL signal. This means that the oxidation of immobilized $Ru(bpy)_3^{2+}$ plays a more important role in the process of ECL than does TPA.[27]

We compared the ECL intensities after 30 min and 1 h incubation for normal amplification and dendritic amplification (data not shown), respectively. In the case of normal amplification, the ECL intensity after 30 min incubation was almost the same as the ECL intensity after 1 h incubation. In the case of dendritic amplification, the ECL intensity after 30 min incubation was slightly lower than the intensity after 1 h incubation. Thus, we concluded that 1 h incubation at 50 °C is sufficient for the DNA hybridization in this experiment.

In our approach, it was possible to hybridize at most five $Probe_{2c}$RSNPs hexagonally with one central $Probe_{1,2}$RSNP, resulting in more enhanced ECL (considering the hexagonal packing mode of RSNPs, four $Probe_{2c}$RSNPs for the sides and one $Probe_{2c}$RSNP for the upper side are available for one $Probe_{1,2}$RSNP after dendritic amplification). We synthesized RSNPs of a uniform size (~60 nm) and functionalized their surfaces with various DNAs for signal amplification. Although the immobilized DNAs were different, the sizes of the resulting RSNPs ($Probe_{1,2}$RSNP and $Probe_{2c}$RSNP) were almost the same (~60 nm). Since $Probe_{1,2}$RSNP and $Probe_{2c}$RSNP are of the same size, we would expect that dendritic amplification could enhance the ECL signal 4~5 times more than normal amplification. Dendritically amplified ECL signals associated with $\mathbf{Probe_{1,2}}$RSNP and $\mathbf{Probe_{2c}}$RSNP were in fact 5 times greater than the normally amplified ECL signals associated with $\mathbf{Probe_{1,2}}$RSNPs. From the 5-fold ECL signal enhancement after dendritic amplification, it can be inferred that there is little steric hindrance between hybridized RSNPs. $\mathbf{Probe_{2c}}$RSNPs are well hybridized with $\mathbf{Probe_{1,2}}$RSNPs and can therefore enhance the ECL signal associated with DNA hybridization.

3. Performance of the ECL-based DNA sensor with dendritic amplification

Fig. 6 shows the correlation between the concentration of the target DNA and the ECL intensity after hybridization with the ECL signal amplifiers ($\mathbf{Probe_{2c}}$RSNPs). The calibration curve between the ECL intensity and the concentration of the target DNA in a logarithmic scale is shown in the inset of Fig. 6. It can be seen that the ECL intensity has a good linear relationship with the concentration of the target DNA. Furthermore, the linear range is wide, extending from 10 fM to 10 pM (slope = 0.097; intercept = 4.07; R^2 = 0.973). While 1 fM of the target DNA could not be detected through normal amplification (data not shown), it was clearly detected using dendritic amplification. As control experiments, we carried out the above mentioned

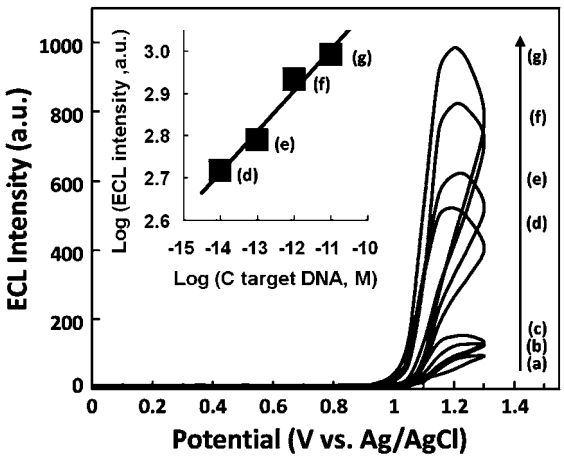

Fig. 6 The ECL profiles of the different concentrations of the target DNA after hybridization with $\mathbf{Probe_{2c}}$RSNP (dendritic amplification). The concentration of the target DNA: (a) no target DNA, (b) non-complementary DNA (10 fM), (c) 1 fM, (d) 10 fM, (e) 100 fM, (f) 1 pM and (g) 10 pM. Other conditions were the same as in Fig. 4. Inset: the logarithmic standard plot.

experiments in the absence of the target DNA and in the presence of non-complementary DNA (10 fM). Both of their ECL intensity showed only a trace of luminescence (Fig. 6 (a), (b)). This result indicates that the dendritic signal amplification method greatly enhances the sensitivity of detecting DNA.

Conclusions

This article describes the development of a novel dendritic signal amplification methodology. Such an analytical strategy relied on the use of DNA base pairing between RSNPs, which can be simply and conveniently self-assembled to achieve highly amplified ECL signals. The performance of this dendritic signal amplification route was demonstrated in connection with the electrochemical sensing of target DNA. Compared to the normal amplification, the dendritic amplification strategy allowed us to show 5 times higher ECL intensity and determine the concentration of the target DNA down to *ca.* 1 fM. The higher sensitivity enabled by the dendritic amplification route was attributed to the additional DNA hybridization between $Probe_{1,2}$RSNP and $Probe_{2c}$RSNP. Consequently, the ECL intensity has a good linear relationship with the concentration of the target DNA. Although still insufficient to detect nonamplified samples of genomic DNA, this dendritic signal amplification protocol might be particularly useful when the yield of the PCR process is limited. Current studies are underway to explore the use of this approach to produce more amplified signals by introducing additional dendritic structure, which can hybridize with $Probe_{2c}$RSNP for greater sensitivity in the detection of target DNA.

Acknowledgements

This work was supported by the KOSEF grant funded by the MEST (No. 2009-0080734), the KRF grant by MOEHRD (KRF-2007-357-C0072), the SRC grant (R11-2005-008-06002-0), and Seoul R&BD (10543). We also acknowledge the BK21 fellowship grants to I.-S.S and M.S.C.

References

1 T. A. Taton, C. A. Mirkin and R. L. Letsinger, *Science*, 2000, **289**, 1757–1760.
2 S. P. A. Fodor, *Science*, 1997, **277**, 393–403.
3 M. Ramsey, *Nat. Biotechnol.*, 1997, **16**, 40–44.
4 S.-J. Park, T. A. Taton and C. A. Mirkin, *Science*, 2002, **295**, 1503–1506.
5 T. G. Drummond, M. G. Hill and J. K. Barton, *Nat. Biotechnol.*, 2003, **21**, 1192–1199.
6 J. Wang, *Anal. Chim. Acta*, 2002, **469**, 63–71.
7 F. Jelen, A. B. Olejniczak, A. Kourilova, Z. J. Lesnikowski and E. Palecek, *Anal. Chem.*, 2009, **81**, 840–844.
8 M. Rodriguez and A. J. Bard, *Anal. Chem.*, 1990, **62**, 2658–2662.
9 J. I. Kim, I.-S. Shin, H. Kim and J.-K. Lee, *J. Am. Chem. Soc.*, 2005, **127**, 1614–1615.
10 I.-S. Shin, J. I. Kim, T. H. Kwon, J. I. Hong, J.-K. Lee and H. Kim, *J. Phys. Chem. C*, 111, pp. 2280–2286.
11 D. Zhu, Y. Tang, D. Xing and W. R. Chen, *Anal. Chem.*, 2008, **80**, 3566–3571.
12 W. Y. Lee and T. A. Nieman, *Anal. Chem.*, 1995, **67**, 1789–1796.
13 J.-K. Lee, S. H. Lee, M. Kim, H. Kim, D. H. Kim and W.-Y. Lee, *Chem. Commun.*, 2003, **13**, 1602–1603.
14 B. A. Gorman, P. S. Francis and N. W. Barnett, *Analyst*, 2006, **131**, 616–639.
15 H. Wei and E. Wang, *TrAC, Trends Anal. Chem.*, 2008, **27**, 447–459.
16 G. M. Greenway, A. Greenwood, P. Watts and C. Wiles, *Chem. Commun.*, 2006, **1**, 85–87.
17 L. Armelao, R. Bertoncello, S. Gross, D. Badocco and P. Pastore, *Electroanalysis*, 2003, **15**, 803–811.
18 Y. Li, H. Qi, F. Fang and C. Zhang, *Talanta*, 2007, **72**, 1704–1709.
19 H. Wang, C. Zhang, Y. Li and H. Qi, *Anal. Chim. Acta*, 2006, **575**, 205–211.
20 Z. Chang, J. Zhou, K. Zhao, N. Zhu, P. He and Y. Fang, *Electrochim. Acta*, 2006, **52**, 575–580.
21 X. Sun, Y. Du, L. Zhang, S. Dong and E. Wang, *Anal. Chem.*, 2007, **79**, 2588–2592.
22 W. Tan, K. Wang, X. He, X. J. Zhao, T. Drake, L. Wang and R. P. Bagwe, *Med. Res. Rev.*, 2004, **24**, 621–638.
23 J. Schmidt, C. Guesdon and R. J. Schomacker, *J. Nanopart. Res.*, 1999, **1**, 267–276.
24 W. Miao, J.-P. Choi and A. J. Bard, *J. Am. Chem. Soc.*, 2002, **124**, 14478–14485.
25 L. Zhang and S. Dong, *Anal. Chem.*, 2006, **78**, 5119–5123.
26 M.-J. Li, Z. Chen, V. W.-W. Yam and Y. Zu, *ACS Nano*, 2008, **2**, 905–912.
27 S. Zanarini, E. Rampazzo, L. D. Ciana, M. Marcaccio, E. Marzocchi, M. Montalti, F. Paolucci and L. Prodi, *J. Am. Chem. Soc.*, 2009, **131**, 2260–2267.
28 Y. Zu and A. J. Bard, *Anal. Chem.*, 2001, **73**, 3960–3964.